



NATIONAL ADVISORY COMMITTEE FOR AERONAUTICS

RESEARCH MEMORANDUM

for the

Air Materiel Command, Army Air Forces

PERFORMANCE OF COMPRESSOR OF XJ-41-V TURBOJET ENGINE

II - STATIC-PRESSURE RATIOS AND LIMITATION OF

MAXIMUM FLOW AT EQUIVALENT COMPRESSOR

SPEED OF 8000 RPM

By Dean M. Dildine and W. Lewis Arthur

INTRODUCTION

At the request of the Air Materiel Command, Army Air Forces, an investigation is being conducted by the NACA Cleveland laboratory to determine the performance characteristics of the compressor of the XJ-41-V turbojet engine. This report is the second in a series presenting the compressor performance and analysis of flow conditions in the compressor. The static-pressure variation in the direction of flow through the compressor and the location and the cause of the maximum flow restriction at an equivalent speed of 8000 rpm are presented.

After the initial runs reported in reference 1, the leading edges of the impeller blades and the diffuser surfaces were found to have been roughened by steel particles from a minor failure of auxiliary equipment. The leading edges of the impeller blades were refinished and all high spots resulting from scratches in the diffuser and the accessible parts of the vaned collector passages were removed. The initial over-all performance and that obtained with the refinished blades are presented.

INSTRUMENTATION AND METHODS

The compressor installation, instrumentation, and test procedures are described in reference 1. In addition to the instrumentation for the determination of the over-all compressor performance, 104 static-pressure measurement stations were provided on the inner and outer walls of the compressor passages. The

static-pressure taps on the inner wall of the compressor were connected to manometer tubes on the outside by copper tubing that went through bulkhead fittings around the shaft housing, as shown in figures 1 and 2. The stations on the outer wall are also indicated in figures 1 and 2. The stations were grouped to determine the following pressure gradients:

1. The gradient in the direction of flow through the compressor (fig. 3)
  - (a) Along the stationary outer wall of the impeller passage (stations 1 to 12)
  - (b) Through the vaneless-diffuser passage (stations 13 to 17)
  - (c) Along a mean flow path through one vaned-collector passage (stations 18 to 27 and I)
2. Peripheral gradients across the vaned-collector passage (fig. 4)
  - (a) Across the entrance to a vaned-collector passage (stations A to F)
  - (b) Across the exit to a vaned-collector passage (stations G to L)
3. Gradient for peripheral symmetry around the compressor (figs. 1 and 2)
  - (a) At the impeller exit on the outer wall (stations 12, 12a, and 12b)
  - (b) At the vaneless-diffuser exit (stations 17a, 17b, 17c, and D)
  - (c) At the vaned-collector exit (stations M to W)

The static-pressure measurement stations are given by group and location in table I.

## RESULTS AND DISCUSSION

Over-all performance characteristics. - A comparison of compressor and collecting-chamber over-all adiabatic efficiencies before and after refinishing of the compressor parts (fig. 5) indicates that

the effect of refinishing on performance was negligible. Data used in this report are from runs made after refinishing.

The adiabatic efficiency and the total-pressure ratio of the compressor at an equivalent speed of 8000 rpm are shown in figure 6. This performance was based on total pressure and temperature at the impeller entrance and at the exit of the simulated burner annulus. The maximum corrected volume flow was 37,630 cubic feet per minute; the peak adiabatic efficiency, 0.787; and the maximum total-pressure ratio, 2.23.

Static-pressure gradients in direction of flow. - The operating points at maximum flow, at peak adiabatic efficiency, and at near surge conditions indicated in figure 6 were chosen for studying the static-pressure variation through the compressor. The static pressures along a flow path through the compressor, expressed as the ratio to the static pressure at the impeller-entrance station, are shown in figure 7 for these three performance conditions. The abscissa designates the stations shown schematically in figure 3 and bears no relation to path length or changes in radius. The pressures on inner and outer walls are plotted separately for the vaneless diffuser and the vaned collector.

At the point of peak adiabatic efficiency, there was a steady static-pressure rise along the stationary impeller shroud and through the vaneless diffuser. In the vaned collector, where the radius increases and then decreases in the direction of flow, the static pressure rose slightly at the entrance and then remained practically constant on the inner and outer walls through the rest of the vaned collector and through the simulated burner annulus at an average pressure of about 2.26.

At low flow near surge, the pressure rise along the impeller stationary shroud was almost as great as at peak efficiency but the pressure rise in the vaneless diffuser was somewhat smaller. There was a sharper rise in pressure at the entrance to the vaned collector at this flow than at peak efficiency. The pressure remained practically constant on the inner and outer walls through the remainder of the vaned collector and through the simulated burner annulus at an average value of 2.07.

At the maximum-flow condition, the pressure ratio dropped slightly at the impeller entrance and then increased until it was equal to the pressure at the impeller tip at peak efficiency. In the vaneless diffuser, the pressure increased to a value higher than at peak efficiency. The static-pressure ratio was 2.09 on both the inner and outer walls at the vaneless-diffuser exit at maximum flow,

whereas at peak efficiency the pressure ratios on the inner and the outer walls were 1.90 and 1.99, respectively. At station 18 in the vaned collector, the static-pressure ratio dropped to about one-fourth that at the vaneless-diffuser exit (about one half the inlet static pressure). This critical pressure drop indicated that a sonic velocity had been reached in this region. The occurrence of a sonic velocity here indicated that the effective flow area was reduced by the occurrence of flow separation near the vaned-collector entrance. The maximum flow of the compressor at an equivalent speed of 8000 rpm was thus limited by a sonic velocity in the entrance of the vaned collector. The static pressure was nearly constant on the inner and outer walls through the part of the vaned collector where the radius of the mean flow path was decreasing in the direction of flow.

Peripheral static-pressure gradients across vaned-collector passage. - The static-pressure-ratio variation across the entrance of one vaned-collector passage, on the inner and outer walls, is shown in figure 8. At all flows the static pressure was greater on the outer wall than on the inner wall over most of the passage width. This condition also existed practically all the way through the compressor in the direction of flow and was due to the centrifugal effect of the rotating air. At peak over-all compressor adiabatic efficiency and at flow near surge, the static pressure increased across the passage entrance in the direction of impeller rotation (stations B to E), as would be expected if the air was entering the passage at the design angle. At maximum flow this pressure gradient had reversed and the pressure was decreasing from station B to E, which indicated that the entrance edges of the collector vanes were no longer operating as airfoils with positive lift. The static-pressure-ratio variation across the exit of one vaned-collector passage is shown in figure 9. The static pressure was generally higher on the outer wall than on the inner wall across the passage exit, as at the entrance, but at peak efficiency and flow near surge these pressure ratios were very nearly the same and were more nearly constant across the passage than at the collector entrance.

Symmetry of static pressure around periphery of compressor. - Static-pressure ratios at four stations around the periphery at the vaned-collector entrance on the inner and outer walls are shown in figure 10. The static-pressure ratios at the exit of each vaned-collector passage on the inner and outer walls are shown in figure 11. The position of these stations in a passage exit is about the same as station I. These curves indicate that the flow was very nearly symmetrical around the periphery of the compressor. The static pressures at stations 12, 12a, and 12b at the impeller exit were also very nearly equal. The measurements taken in one vaned-collector passage or at one set of radial stations in the

vaneless diffuser should therefore be typical of measurements taken at any other position around the periphery.

#### SUMMARY OF RESULTS

An investigation of static pressures in the compressor of the XJ-41-V turbojet engine operating at an equivalent speed of 8000 rpm yielded the following results:

1. The static-pressure ratio in the vaneless diffuser increased as the flow increased for the entire flow range. The static-pressure ratio in the impeller increased as the flow increased from near surge to peak efficiency but remained practically unchanged from peak efficiency to maximum flow.

2. The maximum flow limitation of the compressor was caused by separation, which reduced the effective flow area at the vaneless collector entrance. This reduction of area was so great that a sonic velocity existed in this region.

3. At all flows the static pressure remained practically constant through the part of the vaneless collector where the radius of the mean flow path was decreasing in the direction of flow.

4. The static pressure around the periphery of the impeller exit, vaneless-diffuser exit, and vaneless collector exit is sufficiently symmetrical to indicate that measurements taken in one vaneless collector passage are common to all passages.

Flight Propulsion Research Laboratory,  
National Advisory Committee for Aeronautics,  
Cleveland, Ohio.

*Dean M. Dildine*  
Dean M. Dildine,  
Mechanical Engineer.

W. Lewis Arthur,  
Mechanical Engineer.

Approved:

Robert O. Bullock,  
Mechanical Engineer.

Oscar W. Schey,  
Mechanical Engineer.

jh

## REFERENCE

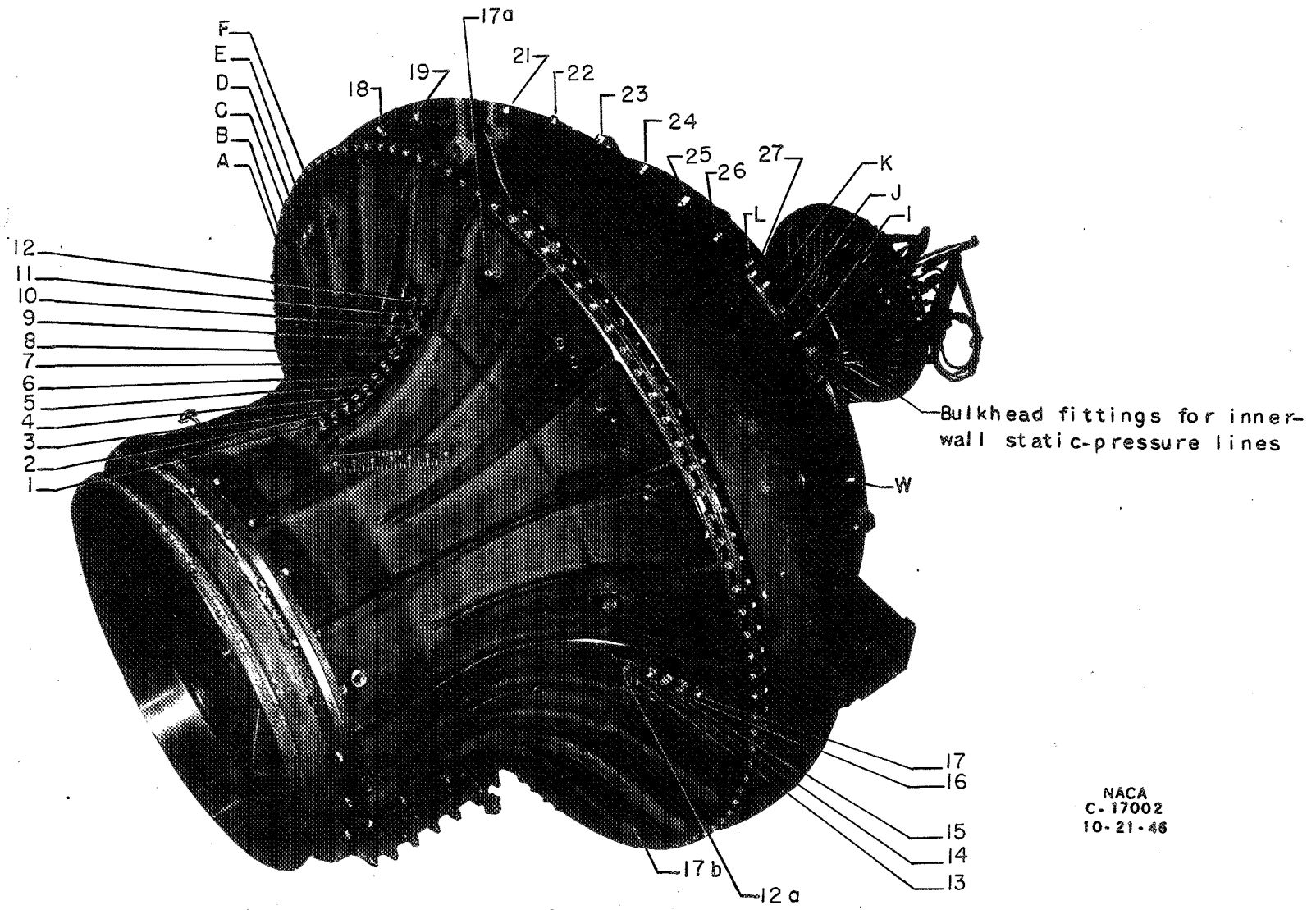
1. Ginsburg, Ambrose, and Creagh, John W. R.: Performance of Compressor of XJ-41-V Turbojet Engine. I - Preliminary Investigation at Equivalent Compressor Speed of 8000 rpm. NACA RM No. E7A17a, Army Air Forces, 1947.

TABLE I - STATIC-PRESSURE MEASUREMENT STATIONS IN COMPRESSOR  
OF XJ-41-V TURBOJET ENGINE

Location	Direction and distribution	Figure	Station	Number on outer wall	Number on inner wall
Along stationary shroud of impeller	Equally spaced along profile in axial plane	1 and 3	1 - 12	12	0
At impeller exit on the outer wall	At the same radial position and 90° on each side of station 12	1	12a and 12b	2	0
On vaneless-diffuser section	Along radial lines 180° apart	1 and 3	13 - 17	10	10
Along passage walls of vaned collector	Following mean flow path along increasing and decreasing radius of vaned collector	1 and 3	18 - 27 and I	10	10
Across entrance to one vaned-collector passage	Spaced across passage entrance in radial plane	1 and 4(a)	A - F	6	6
Across exit to one vaned-collector passage	Evenly-spaced across passage discharge in radial plane	2 and 4(b)	G - L	4	6
Around periphery at vaned-collector entrance	About same position in three passage entrances as station D	1	17a, 17b, and 17c	3	3
Around periphery at vaned-collector exit	In position similar to station I in each passage discharge	2	M - W	11	11

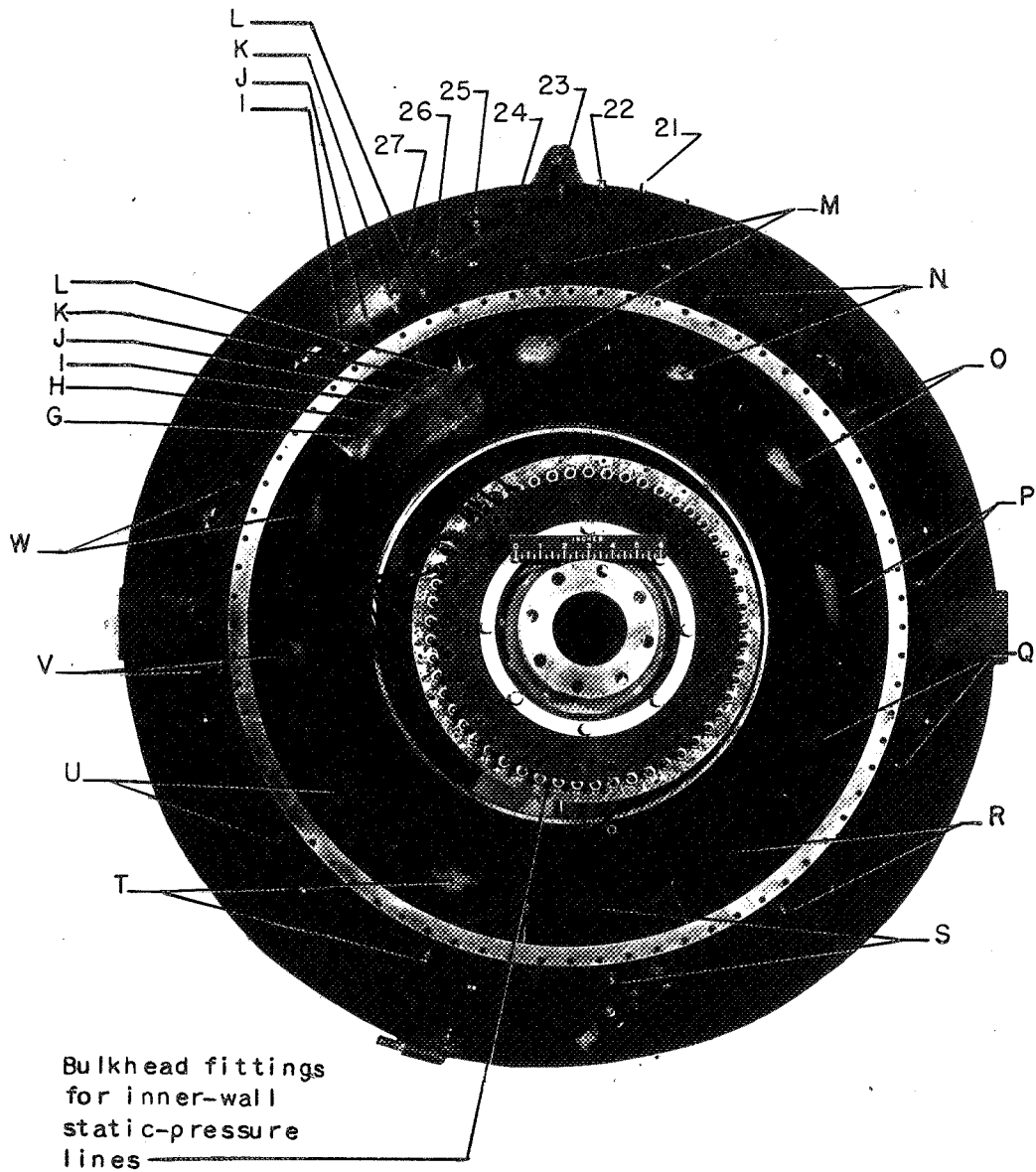


25



NACA  
C-17002  
10-21-46

Figure 1. - Front view of compressor of XJ-41-V turbojet engine showing location of static-pressure stations.



NACA  
C-17004  
10-21-46

Figure 2. - Rear view of compressor of XJ-41-V turbojet engine showing location of static-pressure stations.

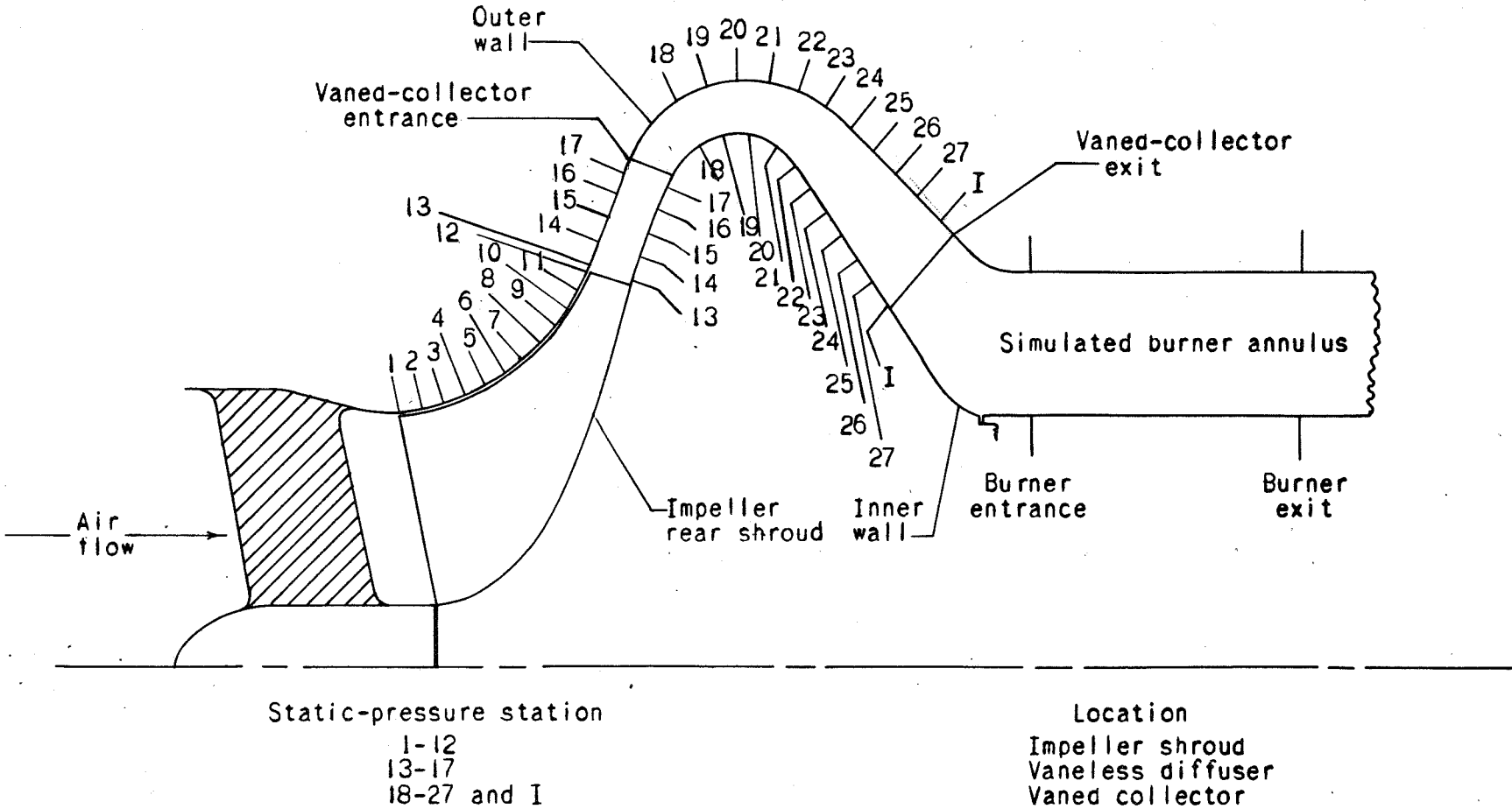
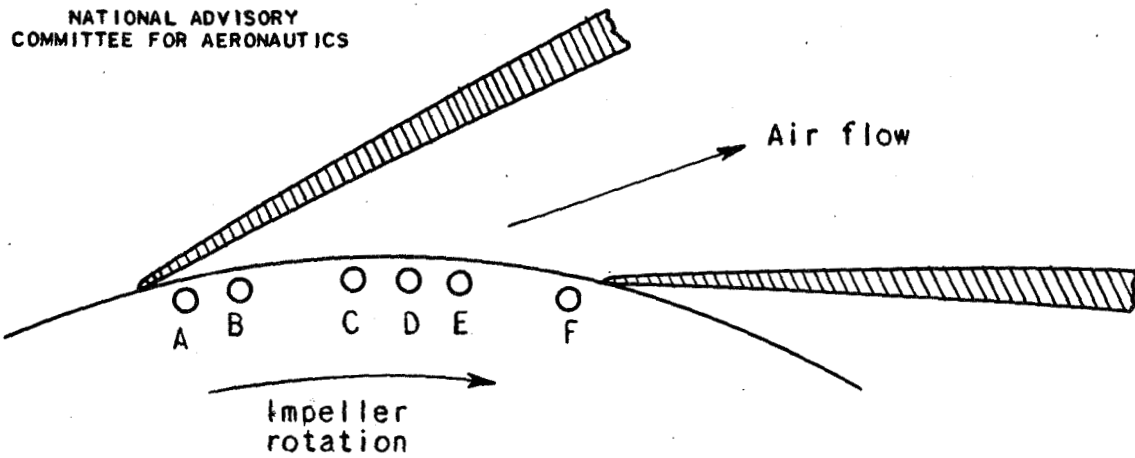
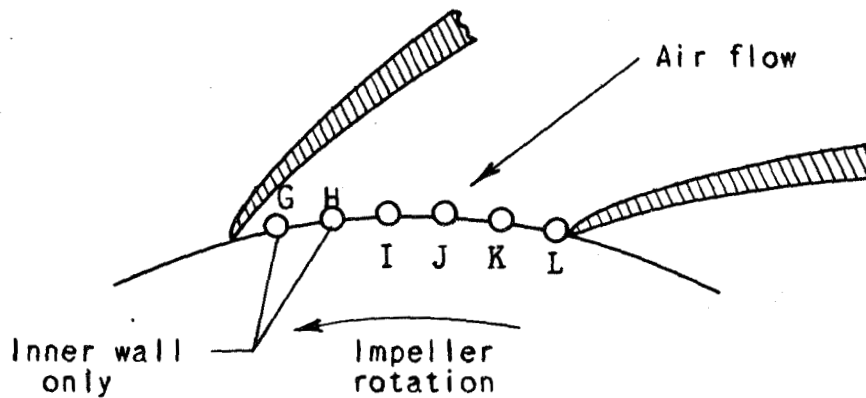


Figure 3. - Location of static-pressure stations in compressor of XJ-41-V turbojet engine.



(a) Vaned-collector entrance normal to flow path.



(b) Vaned-collector exit normal to flow path.

Figure 4. - Static-pressure measuring stations at entrance and exit of one vaned-collector passage.

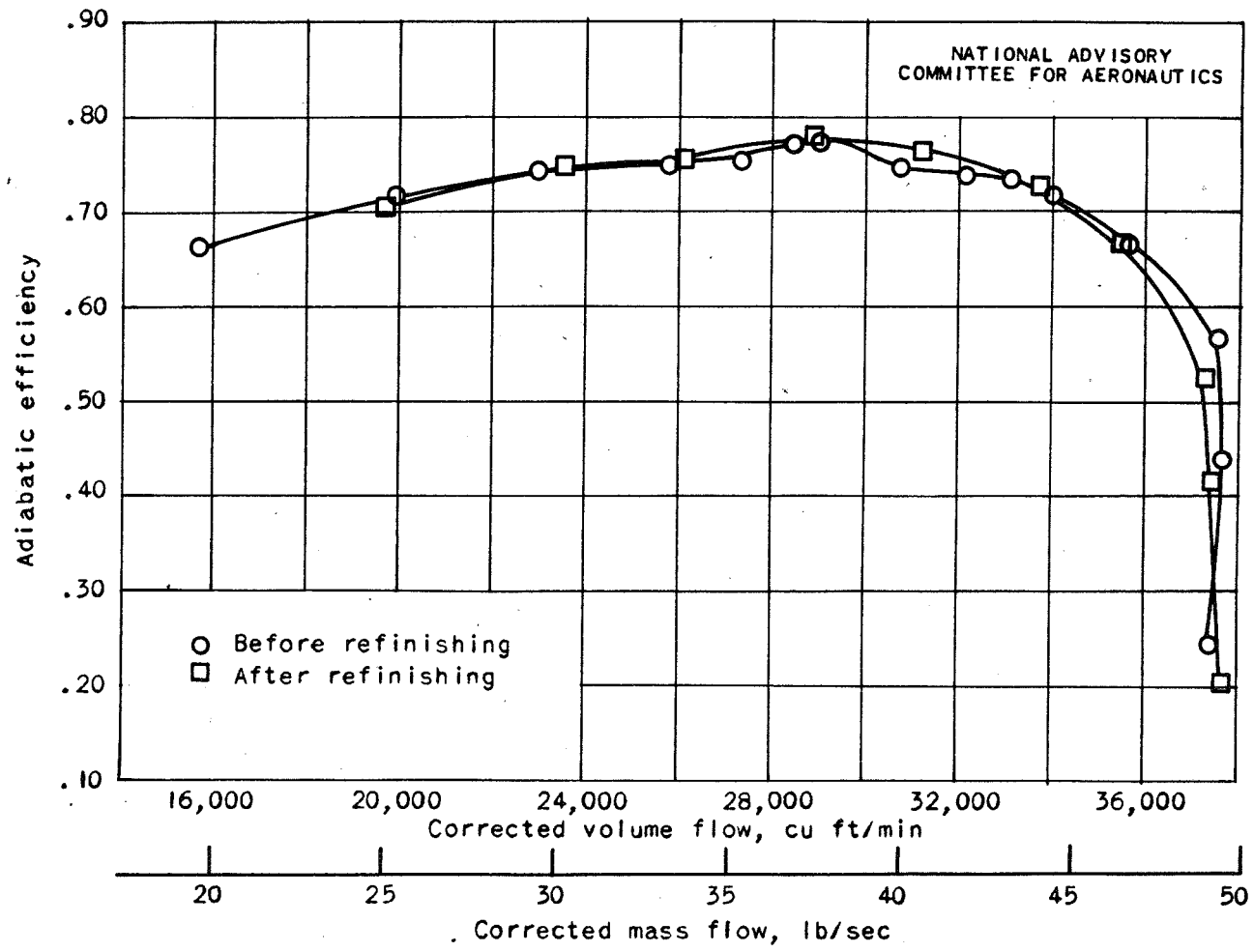


Figure 5. - Compressor and collecting-chamber over-all adiabatic efficiency at equivalent compressor speed of 8000 rpm before and after refinishing compressor parts.

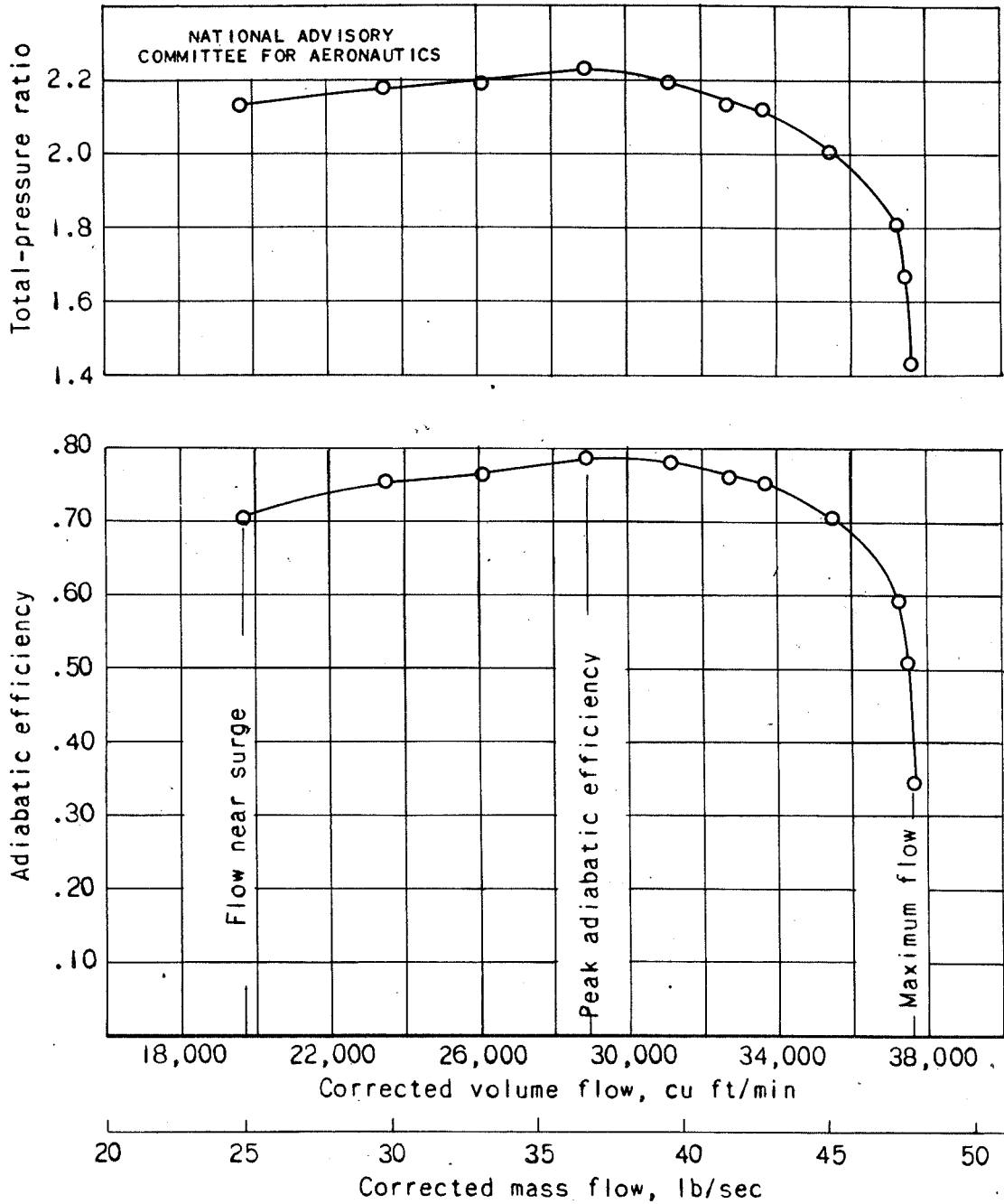


Figure 6. - Compressor over-all total-pressure ratio and adiabatic efficiency at equivalent compressor speed of 8000 rpm.

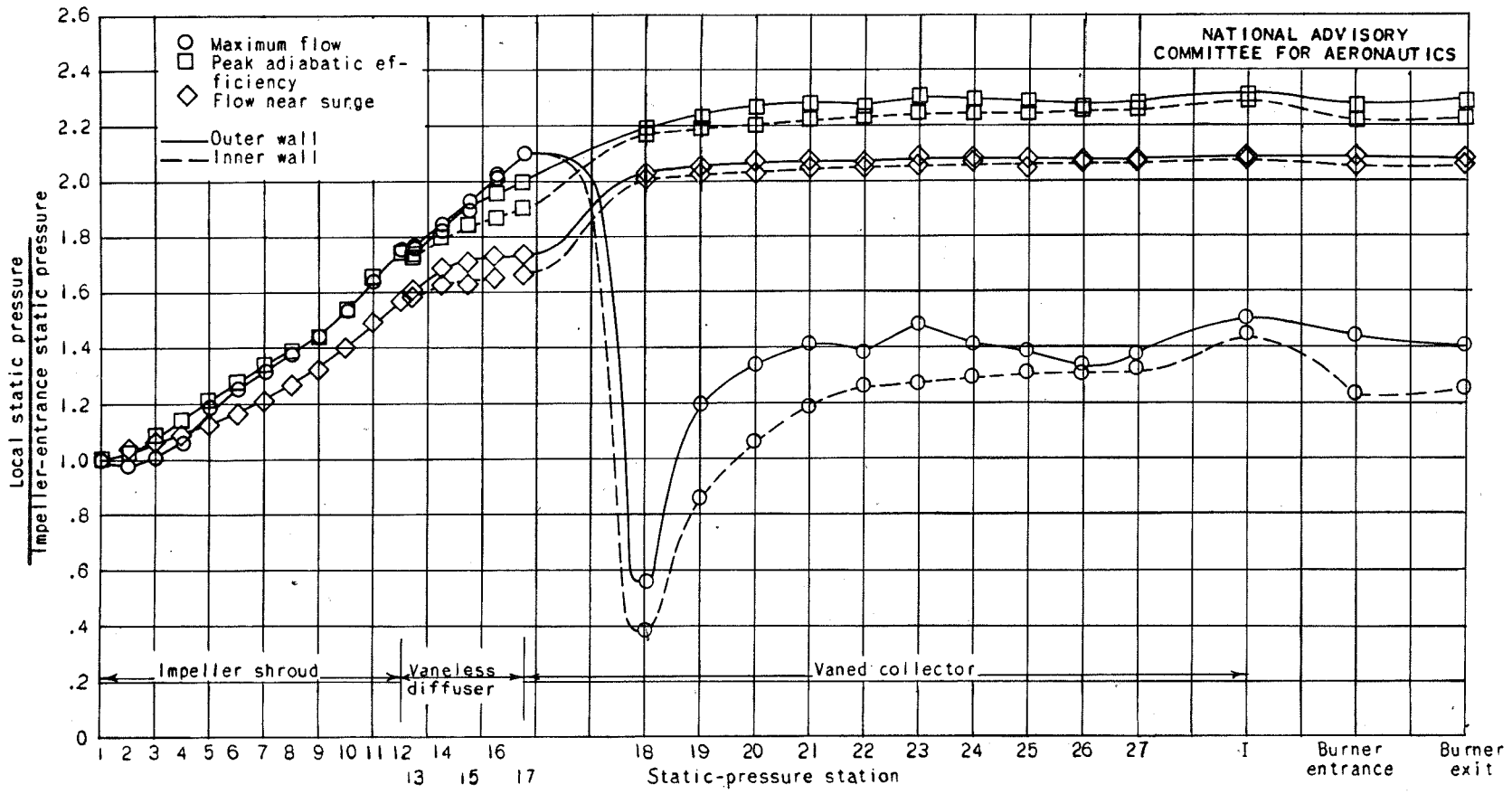


Figure 7. - Static-pressure variation through compressor.

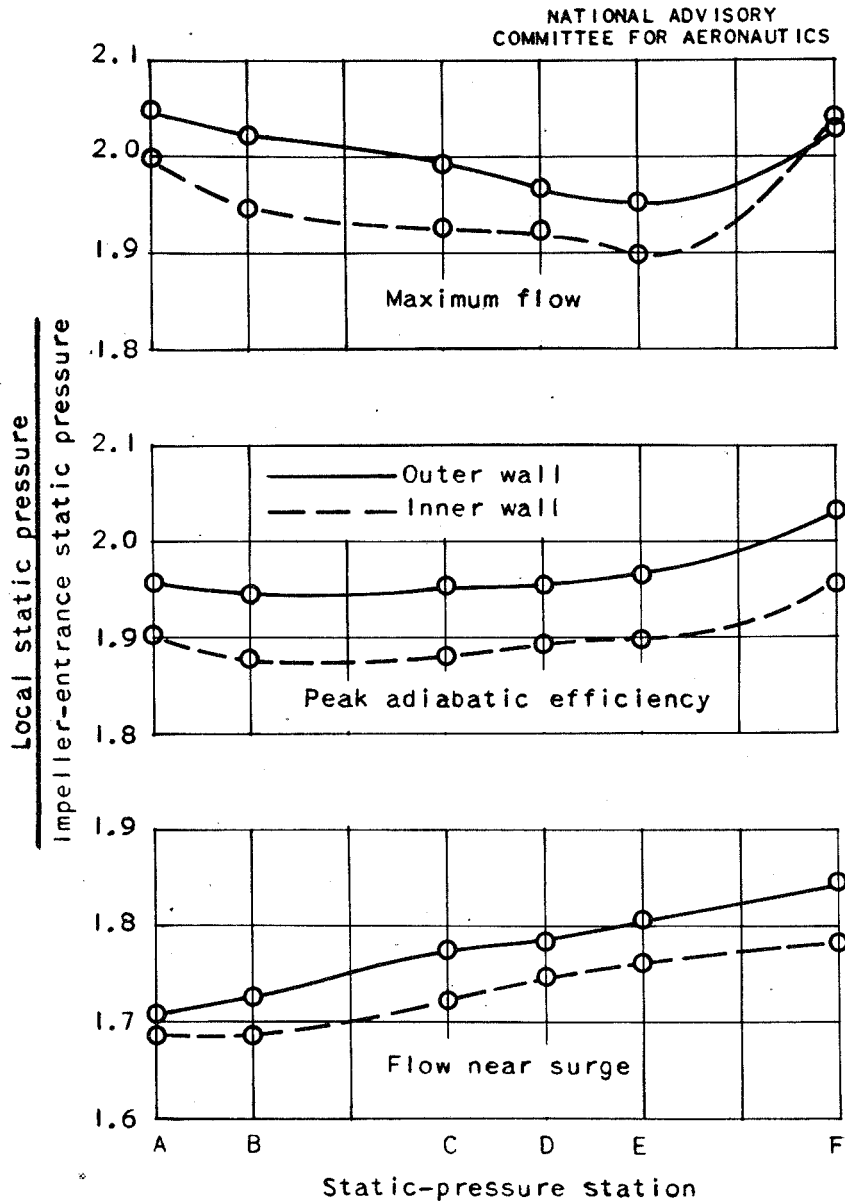


Figure 8. - Static-pressure ratio variation across entrance of one vaned-collector passage.



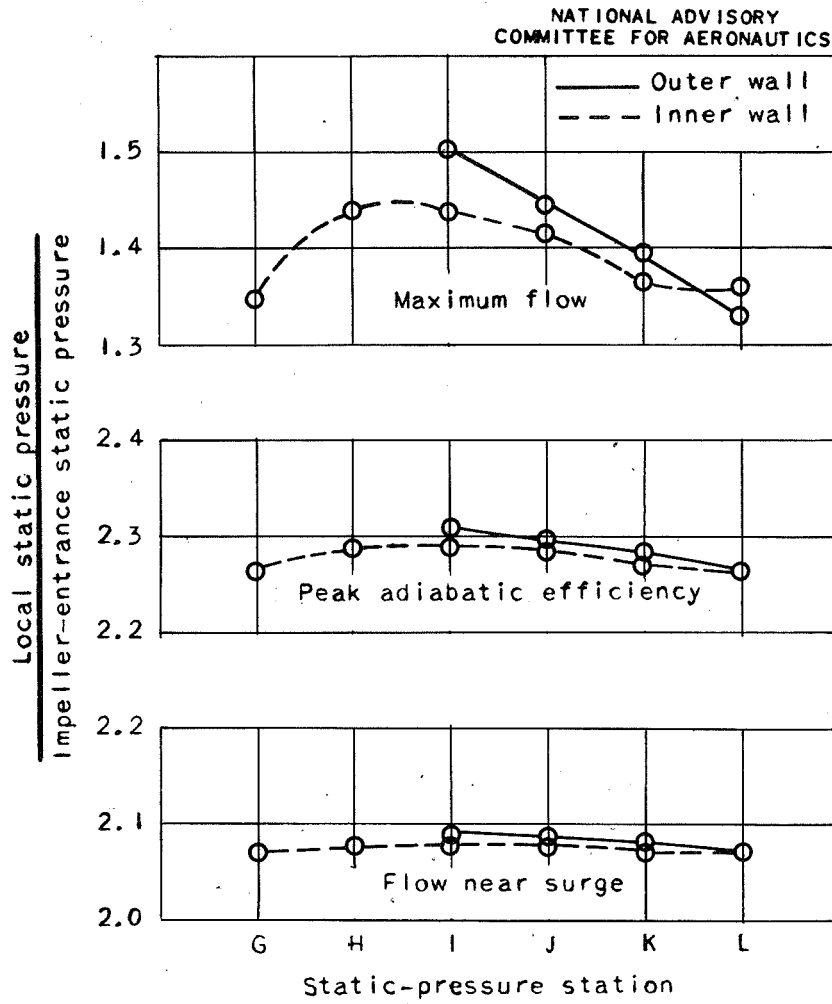


Figure 9. - Static-pressure ratio variation across exit of one vaned-collector passage.

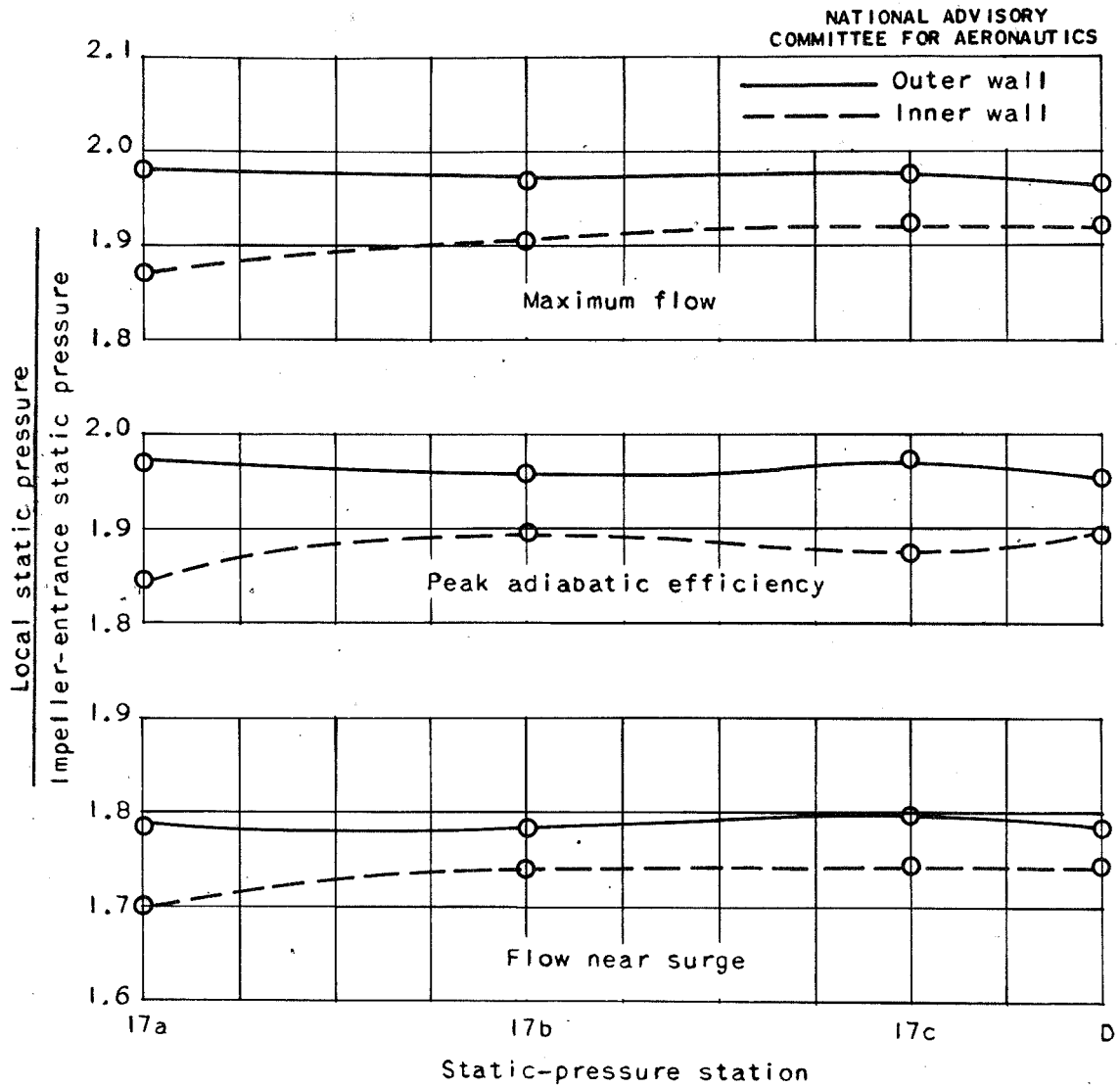


Figure 10. - Static-pressure ratio variation around periphery at vaned-collector entrance.

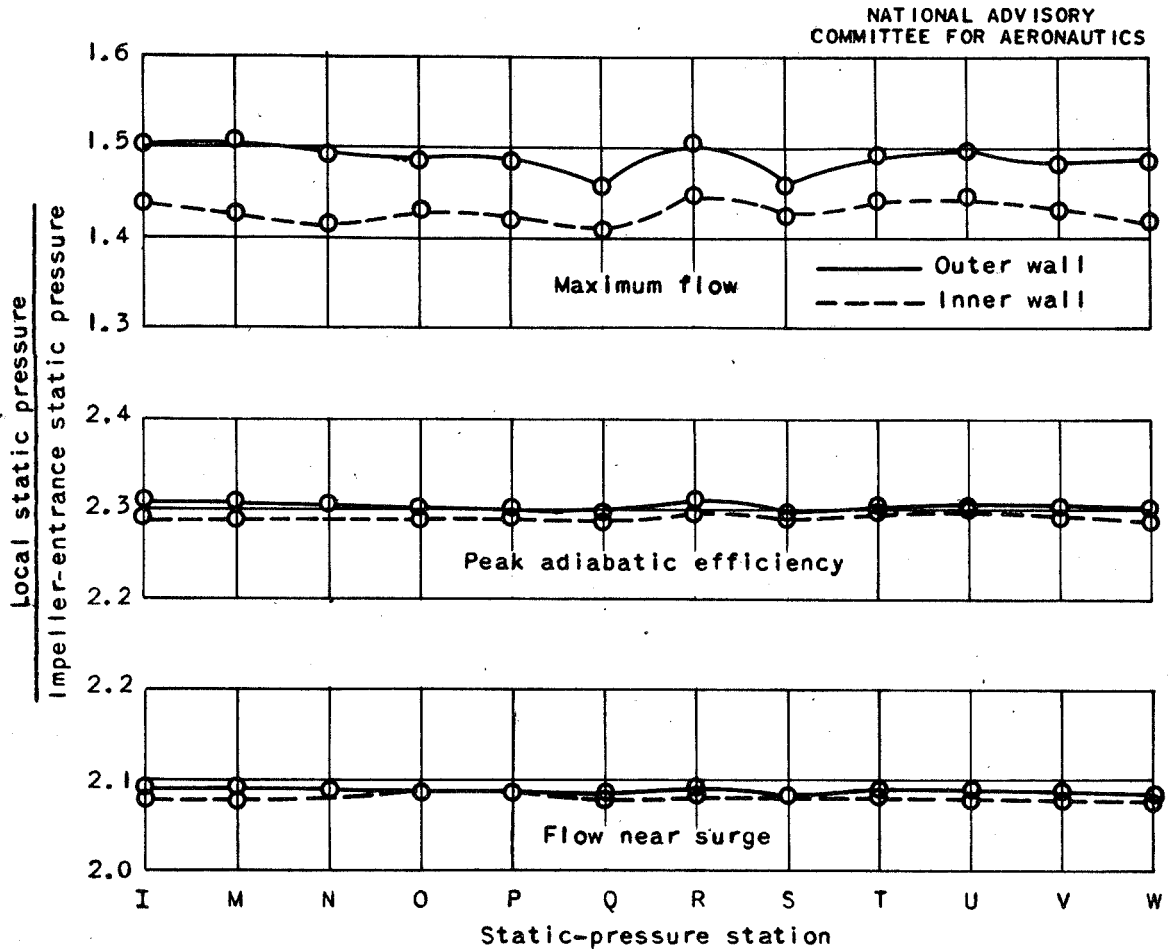


Figure 11. - Static-pressure ratio variation around periphery at vaned-collector exit.

UNCLASSIFIED

UNCLASSIFIED